

Controls on the hydrogen isotope composition in the pore water from the Dajiuhu Peatland, central China

Yuhang WANG¹, Xianyu HUANG (✉)^{1,2}

¹ State Key Laboratory of Biogeology and Environmental Geology, School of Earth Sciences, China University of Geosciences, Wuhan 430074, China

² Hubei Key Laboratory of Critical Zone Evolution, School of Geography and Information Engineering, China University of Geosciences, Wuhan 430078, China

© Higher Education Press 2024

Abstract The hydrogen isotope composition of leaf wax *n*-alkanes ($\delta^2\text{H}_{\text{alk}}$) has been used to reconstruct hydroclimate conditions, yet the factors that influence it are not fully understood, particularly the control of soil pore water $\delta^2\text{H}$. This study monitored the temporal and vertical variations of peat pore water $\delta^2\text{H}$ ($\delta^2\text{H}_{\text{pw}}$) from 2015 to 2019 in the Dajiuhu peatland, central China. Results showed that $\delta^2\text{H}_{\text{pw}}$ was highly variable in the surface layers (0–10 cm; avg. -47‰ , $1\sigma = 11\text{‰}$) and remained almost constant in deeper depths (below 50 cm; avg. -56‰ , $1\sigma = 2\text{‰}$). The $\delta^2\text{H}_{\text{pw}}$ of the 0–10 cm layer was strongly correlated with the preceding month's precipitation $\delta^2\text{H}$ ($\delta^2\text{H}_{\text{p}}$) in the adjacent area ($r = 0.7$, $p < 0.01$), indicating that $\delta^2\text{H}_{\text{p}}$ is the main factor affecting the temporal variations of $\delta^2\text{H}_{\text{pw}}$ in the upper layers. Moreover, the surface (0–10 cm) peat pore water slightly deviated from the local meteoric water line, suggesting that evaporation may also have an effect on the $\delta^2\text{H}_{\text{pw}}$. These findings emphasize the importance of precipitation isotope composition in interpreting the $\delta^2\text{H}_{\text{alk}}$ in peat deposits under subtropical climates.

Keywords pore water, hydrogen isotope composition, spatiotemporal variability, soil evaporation, leaf wax *n*-alkane, peat deposit

1 Introduction

Along with the advance of instrumental techniques over the past decades, the hydrogen isotope compositions ($\delta^2\text{H}$) of leaf wax *n*-alkyl lipids have been increasingly used as a powerful tool for paleohydrological reconstructions (e.g., Sachse et al., 2012; McFarlin et al., 2019; Liu et al., 2022a; Zhao et al., 2022). In the East

Asian summer monsoon regions, the leaf wax *n*-alkane $\delta^2\text{H}$ ($\delta^2\text{H}_{\text{alk}}$) sequences from lacustrine and peat deposits and loess-paleosol sequences have been extensively studied and interpreted as a reflection of variations in precipitation isotope compositions and associated monsoon activities (e.g., Liu and Huang, 2005; Rao et al., 2016; Wang et al., 2021; Zhao et al., 2021; Zhao et al., 2022; Huang et al., 2023). Nonetheless, the effects on the paleo applications of $\delta^2\text{H}_{\text{alk}}$ in natural archives are not fully understood (Sachse et al., 2012; Liu and An, 2018).

Investigations into modern processes have revealed that the $\delta^2\text{H}_{\text{alk}}$ is mainly affected by three factors: the $\delta^2\text{H}$ of precipitation ($\delta^2\text{H}_{\text{p}}$) (Liu and An, 2018; McFarlin et al., 2019), the evaporation of soil water and the transpiration of plants (Feakins and Sessions, 2010; Kahmen et al., 2013), and the fractionation of isotopes during wax biosynthesis (Sachse et al., 2012; Liu and An, 2019; Liu and Liu, 2019). Significant attention has been focused on the impacts of $\delta^2\text{H}_{\text{p}}$ (Sachse et al., 2012; McFarlin et al., 2019) and plant types (Liu and Yang, 2008; Liu et al., 2022a) on $\delta^2\text{H}_{\text{alk}}$; however, the influence of soil water evaporation has not been extensively studied. It is postulated that soil water evaporation leads to an enrichment of deuterium, thus causing a more positive $\delta^2\text{H}_{\text{alk}}$ (Gibson et al., 2008). Some studies suggest that the effect of soil water evaporation on $\delta^2\text{H}_{\text{alk}}$ is insignificant even in arid conditions due to the water absorption through deep roots (Dawson, 1993; Feakins and Sessions, 2010). In contrast, other studies indicate that the impact of evaporation on the $\delta^2\text{H}$ of soil water ($\delta^2\text{H}_{\text{sw}}$) can reach deeper depths (even > 150 cm) in arid settings (Sprenger et al., 2016) and become weaker with increased depth (Dai et al., 2020, 2022). Furthermore, the $\delta^2\text{H}_{\text{alk}}$ sedimentary sequence in peat deposits supports the notion that evaporation may have an effect during long-term drying periods (Huang et al., 2018; Wang et al., 2022). To date, the $\delta^2\text{H}_{\text{sw}}$ variations over long periods of time have not been widely examined.

Received February 14, 2023; accepted July 21, 2023

E-mail: xyhuang@cug.edu.cn

Peat pore water in peatlands offers an interesting chance to investigate the spatial and temporal variations of $\delta^2\text{H}_{\text{sw}}$. Peat deposits have been widely studied to reconstruct paleoclimate through lipid proxies, such as $\delta^2\text{H}_{\text{alk}}$ (e.g., Xie et al., 2000; Seki et al., 2011; Huang et al., 2018), and are suitable for exploring the effect of soil water evaporation on $\delta^2\text{H}_{\text{alk}}$ (Huang and Meyers, 2019). Moreover, the high moisture content in peatlands makes it easy to obtain pore water even during periods of drought. The Dajiuhu peatland, a typical subtropical peatland, has a number of studies conducted on it to explore the influence of evaporation on $\delta^2\text{H}_{\text{sw}}$ over a long-term series. These include sedimentary $\delta^2\text{H}_{\text{alk}}$ (Huang et al., 2018; Yang et al., 2023), physicochemical properties of peat pore water (Zhang et al., 2022), and meteorological and hydrological monitoring (Yang et al., 2024).

This study seeks to examine the spatial and temporal features of $\delta^2\text{H}_{\text{pw}}$ in Dajiuhu peatland, and explore the possible controlling factors (e.g., local conditions, $\delta^2\text{H}_{\text{p}}$, evaporation) that may influence the spatiotemporal variations of $\delta^2\text{H}_{\text{pw}}$, based on the monitoring program conducted in this peatland from 2015 to 2019.

2 Materials and methods

2.1 Study area

The Dajiuhu basin (31°28' N, 110°00' E, 1700 m above the sea level) is located at the western edge of the Shennongjia Forest District, Hubei Province, central China (Fig. 1). This site was designated as an internationally important wetland by the Ramsar Convention in late 2013. Dajiuhu peatland spans an area of 7.5 km², with a typical peat thickness of 2 m (Huang et al., 2017). The dominant peat-forming plants in this peatland are *Sphagnum palustre* and graminoids (Zhao et al., 2018). The climate is mainly characterized by the Asian monsoon, with a mean annual air temperature of 7.2°C and a mean annual precipitation of 1560 mm (Huang et al., 2017).

2.2 Sampling

In 2014, 15 sites were selected for long-term monitoring of hydrological regimes and biogeochemical processes (Table 1; Fig. 1; Huang et al., 2017). These sites were chosen to represent a range of water levels and are less impacted by anthropogenic influences (Huang et al., 2017; Yang et al., 2024). MacroRhizon soil solution samplers (Rhizosphere Research Products B.V., The Netherlands) were installed at seven depths (0–10, 20–30, 50–60, 80–90, 100–110, 120–130, 150–160 cm) to collect peat pore water samples. From 2015 to 2019, peat pore water samples were taken in spring (April,

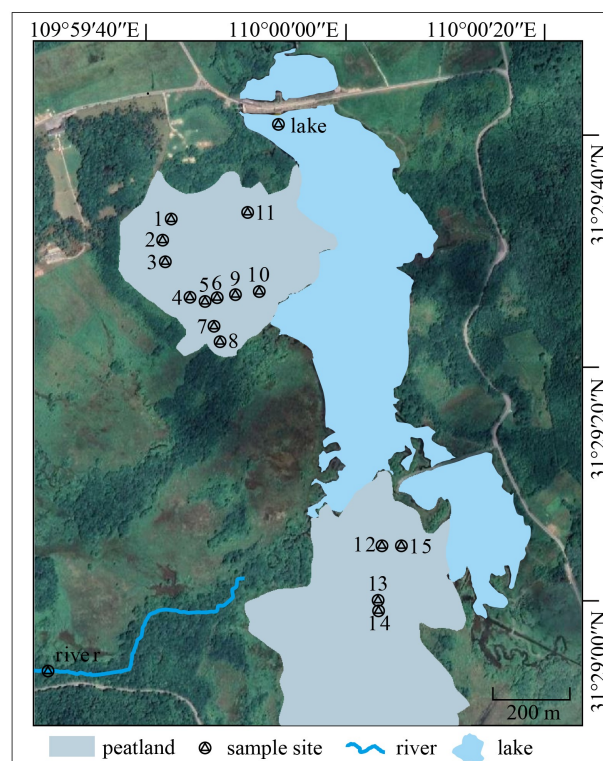


Fig. 1 Map of the Dajiuhu peatland. Monitoring sites were presented by triangles embedded in circles.

Table 1 Locations and the 2015–2019 averaged DWT values (the depth of peat surface to the water table) of the monitoring sites in the Dajiuhu peatland

Monitoring sites	Latitude/ N	Longitude/ E	DWT (mean \pm 1 σ , cm)	Elevation/m
1	31°29'33.24"	109°59'42.54"	0.6 \pm 8.8	1756.5
2	31°29'31.50"	109°59'41.62"	-16 \pm 9.1	1756.8
3	31°29'29.60"	109°59'41.82"	4.1 \pm 4.8	1757.1
4	31°29'26.58"	109°59'44.40"	5.1 \pm 4.4	1755.8
5	31°29'26.26"	109°59'45.97"	4.1 \pm 7.3	1754.6
6	31°29'26.62"	109°59'47.00"	-8.2 \pm 5.2	1754.9
7	31°29'24.14"	109°59'46.72"	-5.1 \pm 9.4	1753.8
8	31°29'22.83"	109°59'47.42"	6.8 \pm 7.6	1754.3
9	31°29'26.86"	109°59'48.86"	17.4 \pm 4.1	1754.6
10	31°29'27.15"	109°59'51.26"	4.9 \pm 9.1	1754.0
11	31°29'33.81"	109°59'50.04"	-3.0 \pm 5.8	1754.6
12	31°29'5.53"	110°00'3.68"	-2.6 \pm 3.7	1753.7
13	31°29'0.90"	110°00'3.23"	5.5 \pm 19	1754.2
14	31°29'0.05"	110°00'3.41"	1.1 \pm 3	1754.4
15	31°29'5.56"	110°00'5.59"	-2.8 \pm 5.7	1753.8
river	31°28'53.24"	109°59'29.92"	-	-
lake	31°29'41.24"	109°59'53.45"	-	-

Notes: ' σ ' represents the standard deviation of DWT. Negative value means water table above the peat surface while positive value means water table below the peat surface. '-' represents no data.

May), summer (June, July, August) and autumn (September, October) of each year.

Three parallel samples of the river and lake water were collected directly from the lake and river connected to the peatland. The river site is located upstream, while the lake site is the water outlet of lake groups. The river and lake water samples were put into 50 mL polyethylene tubes and filtered with 0.45 μm filter membranes before being subjected to instrumental analysis. In 2017, no river and lake samples were taken.

2.3 Instrumental analysis

The isotope compositions of water samples were determined using a liquid water isotope analyzer (IWA-35-EP, Los Gatos Research, USA) at the State Key Laboratory of Biogeology and Environmental Geology, China University of Geosciences, Wuhan. The analytical precision is $\pm 0.6\text{‰}$ for $\delta^2\text{H}$ and $\pm 0.2\text{‰}$ for $\delta^{18}\text{O}$. Isotope results were normalized against Vienna Standard Mean Ocean Water (V-SMOW).

2.4 Statistical analysis

The local meteoric water line (LMWL) and line-conditioned excess (lc-excess) were calculated to evaluate the effect of evaporation on $\delta^2\text{H}_{\text{pw}}$. The LMWL in the

Shennongjia Forest District was determined to be $\delta^2\text{H} = 8.25 \times \delta^{18}\text{O} + 17.14$ (Wang, 2021). The lc-excess represents the deviations between water samples and LMWL in the dual-isotope plots (Landwehr and Coplen, 2006). The expression is as follows:

$$\text{lc-excess} = \delta^2\text{H} - a \times \delta^{18}\text{O} - b, \quad (1)$$

where a represents the slope and b represents the intercept of LMWL. According to the LMWL in the Shennongjia Forest District, the lc-excess of collected water samples was calculated as

$$\text{lc-excess} = \delta^2\text{H} - 8.25 \times \delta^{18}\text{O} - 17.14. \quad (2)$$

Correlation analysis and the Pearson significance test were conducted in the R platform (R Core Team, 2022) with the “corrplot” package (Wei and Simko, 2021).

3 Results

3.1 Meteorological data

Meteorological data between 2015 and 2019 in the Dajiuhu peatland have been published in previous studies (Huang and Meyers, 2019; Yang et al., 2024; Fig. 2). On average, the air temperature was relatively high in

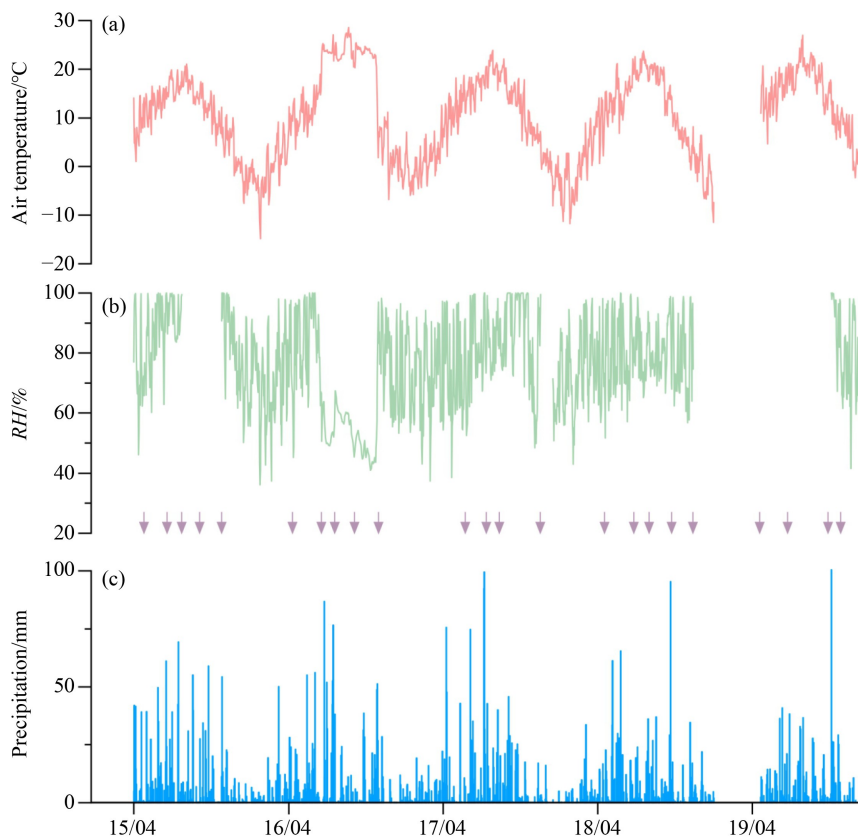


Fig. 2 Variations of meteorological data between 2015 and 2019 in the Dajiuhu peatland. (a) Daily air temperature. (b) Daily RH. (c) Daily precipitation. The purple arrowheads mark the sampling date.

summer (avg. 19°C) and low in winter (avg. -2°C). Rainfall mainly occurred between April and October. The relative humidity (*RH*) kept above 70% for the most time period. During 2015–2019, the mean annual air temperature ranged from 8.3°C to 11.2°C (Fig. 2(a)). The mean annual precipitation ranged from 1497 to 1710 mm (Fig. 2(b)). Notably, the *RH* dropped to 68% during the dry period in the summer of 2016 (Fig. 2(c)).

3.2 $\delta^2\text{H}$ of peat pore water

The $\delta^2\text{H}_{\text{pw}}$ in the upper layers (< 50 cm) became more negative and less variable as the depth increased. The $\delta^2\text{H}_{\text{pw}}$ in the uppermost layer (0–10 cm) had the most variation, ranging from -69‰ to -29‰, and had an average value of -47‰ (Table 2; Fig. 3(a)). The layer of 20–30 cm had slightly smaller fluctuations of $\delta^2\text{H}_{\text{pw}}$ (-58‰ - -46‰, avg. -51‰; Table 2; Fig. 3(a)). In contrast, the lower peat layers (> 50 cm) displayed more

negative $\delta^2\text{H}_{\text{pw}}$ and remained relatively constant over the five-year study period (-58‰ - -54‰; Table 2; Fig. 3(b)).

Over the period from April 2015 to October 2019, the $\delta^2\text{H}_{\text{pw}}$ at 0–10 cm depth ($\delta^2\text{H}_{0-10\text{ cm}}$) from the 15 monitoring sites displayed a variation of less than 12‰ (variance, 1σ) at the same sampling time (Table 2). Additionally, strong positive correlations for the $\delta^2\text{H}_{0-10\text{ cm}}$ ($r > 0.6$, $p < 0.05$) were observed among different sites (Fig. 4). Regarding the layer of 20–30 cm, the $\delta^2\text{H}_{\text{pw}}$ from the 15 monitoring sites fluctuated by less than 9‰ at the same sampling period (Table 2).

Seasonal variations in the averaged $\delta^2\text{H}_{0-10\text{ cm}}$ are evident. In Spring (April, May) and early Summer (June), the $\delta^2\text{H}_{0-10\text{ cm}}$ ranged from -51‰ to -29‰ and were higher than in the following seasons. Exceptions appeared in September 2015 and 2016, with relatively positive values of -47‰ and -50‰ (Fig. 3(a)). On the annual time scale, the averaged $\delta^2\text{H}_{0-10\text{ cm}}$ for 2015 and 2019

Table 2 Results of averaged $\delta^2\text{H}_{\text{pw}}$, $\text{lc-excess}_{0-10\text{cm}}$, mean annual air temperature (*T*), annual precipitation (*P*), and the annual relative humidity (*RH*)

Year/month	$\delta^2\text{H}_{\text{pw}}$ (mean \pm 1 σ ; ‰)									Lc-excess 0–10 cm	<i>T</i> /°C	<i>P</i> /mm	<i>RH</i> /%
	0–10	20–30	50–60	80–90	100–110	120–130	150–160	river	lake				
15/04	-38 \pm 5	-	-	-	-	-	-	-54	-44	-	-	-	-
15/06	-29 \pm 10	-50 \pm 3	-56 \pm 2	-	-57 \pm 2	-	-57 \pm 2	-39	-48	-1.0	-	-	-
15/07	-49 \pm 4	-50 \pm 3	-57 \pm 2	-	-57 \pm 2	-	-54 \pm 6	-54	-51	-3.2	8.3	1643.2	81*
15/09	-47 \pm 4	-51 \pm 4	-56 \pm 3	-	-56 \pm 1	-	-58 \pm 1	-55	-49	-5.0	-	-	-
15/10	-53 \pm 4	-50 \pm 3	-55 \pm 3	-	-56 \pm 2	-	-57 \pm 2	-	-	-3.4	-	-	-
16/04	-37 \pm 5	-49 \pm 1	-55 \pm 2	-57 \pm 2	-57 \pm 2	-57 \pm 2	-58 \pm 2	-49 \pm 0	-42 \pm 1	1.4	-	-	-
16/06	-37 \pm 5	-46 \pm 2	-54 \pm 3	-57 \pm 2	-57 \pm 2	-57 \pm 2	-57 \pm 2	-48 \pm 0	-41 \pm 1	0.2	-	-	-
16/07	-58 \pm 9	-46 \pm 9	-55 \pm 3	-57 \pm 3	-58 \pm 2	-58 \pm 2	-58 \pm 2	-79 \pm 0	-61 \pm 0	-2.0	11.2	1710.0	68
16/09	-50 \pm 5	-53 \pm 9	-55 \pm 3	-57 \pm 3	-58 \pm 2	-58 \pm 2	-58 \pm 2	-	-	-5.3	-	-	-
16/10	-67 \pm 9	-51 \pm 4	-55 \pm 3	-57 \pm 2	-58 \pm 2	-58 \pm 2	-58 \pm 2	-64	-65	-0.8	-	-	-
17/05	-35 \pm 5	-49 \pm 3	-55 \pm 3	-	-	-	-	-	-	-2.7	-	-	-
17/07	-46 \pm 12	-49 \pm 2	-56 \pm 1	-	-	-	-	-	-	-4.0	9.0	1682.1	78
17/08	-61 \pm 5	-49 \pm 5	-54 \pm 3	-	-	-	-	-	-	-5.2	-	-	-
17/11	-69 \pm 6	-58 \pm 4	-54 \pm 3	-	-	-	-	-	-	-2.2	-	-	-
18/04	-52 \pm 8	-57 \pm 4	-56 \pm 3	-	-56 \pm 2	-	-	-63 \pm 1	-52 \pm 1	-1.0	-	-	-
18/06	-37 \pm 4	-58 \pm 4	-57 \pm 3	-	-57 \pm 2	-	-	-57 \pm 1	-47 \pm 0	-2.1	-	-	-
18/08	-50 \pm 6	-56 \pm 4	-56 \pm 3	-	-56 \pm 2	-	-	-52 \pm 3	-47 \pm 0	-1.8	8.3	1497.1	78
18/09	-54 \pm 3	-57 \pm 3	-57 \pm 1	-	-58 \pm 2	-	-	-55 \pm 1	-53 \pm 1	-2.7	-	-	-
18/11	-57 \pm 4	-55 \pm 2	-55 \pm 2	-	-57 \pm 2	-	-	-58 \pm 1	-54 \pm 0	-1.6	-	-	-
19/04	-39 \pm 7	-53 \pm 4	-55 \pm 3	-	-56 \pm 3	-	-	-52 \pm 0	-42 \pm 1	1.4	-	-	-
19/06	-32 \pm 4	-50 \pm 7	-55 \pm 3	-	-57 \pm 2	-	-	-48 \pm 0	-40 \pm 0	0.1	13.3*	1060.5*	80*
19/09	-37 \pm 3	-47 \pm 5	-53 \pm 3	-	-	-	-	-46 \pm 0	-41 \pm 0	-1.5	-	-	-
19/10	-43 \pm 4	-48 \pm 6	-54 \pm 2	-	-	-	-	-51 \pm 1	-49 \pm 0	0.6	-	-	-

Notes: ‘ σ ’ is the standard deviation of $\delta^2\text{H}$. ‘-’ represents that data are not available. ‘*’ means that the data are incomplete.

were -43‰ and -37‰ , respectively, which were higher than those in other monitoring years (-50‰ – -53‰) (Fig. 3(a)). In comparison, the temporal variations of $\delta^2\text{H}_{20-30\text{ cm}}$ were less pronounced (avg. -51‰ , $1\sigma = 4\text{‰}$).

3.3 $\delta^2\text{H}$ of the river and lake water

During 2015–2019, the $\delta^2\text{H}$ of river samples ($\delta^2\text{H}_{\text{river}}$) ranged from -79‰ to -39‰ , whereas the $\delta^2\text{H}$ of lake samples ($\delta^2\text{H}_{\text{lake}}$) fluctuated between -65‰ and -40‰ (Fig. 3(c)). Generally, $\delta^2\text{H}_{\text{lake}}$ was the highest in June (except for July 2015) yet the lowest in the last sampling month of each year. The temporal patterns of $\delta^2\text{H}_{\text{river}}$ and $\delta^2\text{H}_{\text{lake}}$ were similar across the sampling period and had a strong correlation with the averaged $\delta^2\text{H}_{0-10\text{ cm}}$ ($r > 0.46$) (Fig. 4).

4 Discussion

4.1 Controls on spatial and vertical variations of $\delta^2\text{H}_{\text{pw}}$

The $\delta^2\text{H}_{\text{pw}}$ in the peat profiles of the Dajiuhu peatland decrease with increasing depth, with mean values ranging from -47‰ to -56‰ and deviation decreasing from 11‰ to 2‰ (Fig. 3). This vertical pattern is likely the result of two factors: soil evaporation in shallow layers and long residence time in deeper layers (Sprenger et al., 2016; Dai et al., 2020). Surface $\delta^2\text{H}_{\text{pw}}$ is usually affected by evaporation, leading to higher values due to kinetic effects (Gibson et al., 2008). With increasing depth, the

influence of soil evaporation diminishes, resulting in less enrichment of ^2H . This is evident in the dual-isotope plot, where the isotope data of soil water influenced by evaporation is plotted on the lower right of the LMWL, with slight deviations of surface (0–10 cm) peat pore water from the LMWL (Fig. 5). The influence depth is limited in the top peat layers (0–10, 20–30 cm) in the Dajiuhu peatland and shallower than in other locations (Sprenger et al., 2016), which is likely due to the humid climate and water table close to the ground surface. The $\delta^2\text{H}_{\text{pw}}$ in the Dajiuhu peatland does not show an abrupt change, indicating that preferential flow is not the primary factor for the vertical variations of $\delta^2\text{H}_{\text{pw}}$ (Pu et al., 2020).

The distribution of the averaged $\delta^2\text{H}_{\text{pw}}$ along depths is mainly shaped by evaporation, but the magnitude of the $\delta^2\text{H}_{\text{pw}}$ changes at different depths is mainly a consequence of the mixing of multiple precipitations, as evidenced by the nearly constant $\delta^2\text{H}_{\text{pw}}$ ($\sim -57\text{‰}$) in deeper depths (50–60, 80–90, 100–110, 120–130, 150–160 cm). Studies have indicated that $\delta^2\text{H}_{\text{p}}$ may vary with rain events (Dai et al., 2020) and differ significantly between seasons (Wang et al., 2020). This is why the $\delta^2\text{H}_{0-10\text{ cm}}$ exhibits the highest variation (-69‰ to -29‰) due to the direct influence of precipitation. In the deeper peat layers (20–30, 50–60, 80–90, 100–110, 120–130, 150–160 cm), the $\delta^2\text{H}_{\text{pw}}$ is affected by the mixing of prior precipitation (Allen et al., 2014; Xu et al., 2022) and thus becomes less variable. Jung et al. (2022) observed that the $\delta^2\text{H}$ of groundwater across South Korea was mainly recharged by precipitation during the rainy season. In

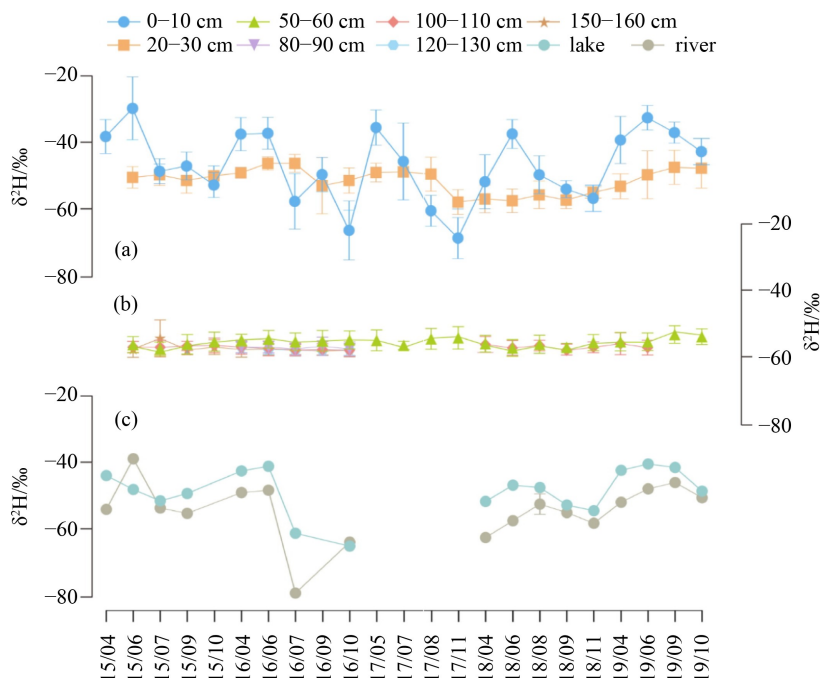


Fig. 3 Variations of water $\delta^2\text{H}$ between 2015 and 2019 in the Dajiuhu peatland. (a) $\delta^2\text{H}_{\text{pw}}$ in the depths of 0–10 and 20–30 cm. (b) $\delta^2\text{H}_{\text{pw}}$ in the depths of 50–60, 80–90, 100–110, 120–130, and 150–160 cm. (c) $\delta^2\text{H}$ of river and lake water.

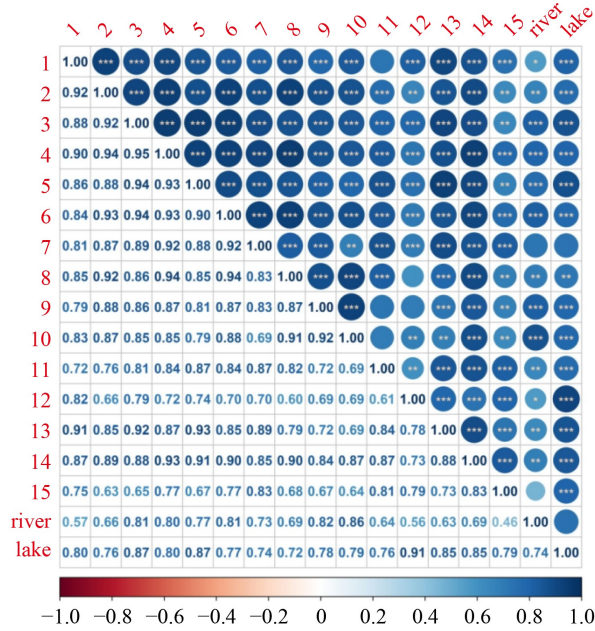


Fig. 4 Correlations among $\delta^2\text{H}_{0-10\text{ cm}}$ from peatland monitoring sites, $\delta^2\text{H}_{\text{river}}$ and $\delta^2\text{H}_{\text{lake}}$ between 2015 and 2019.

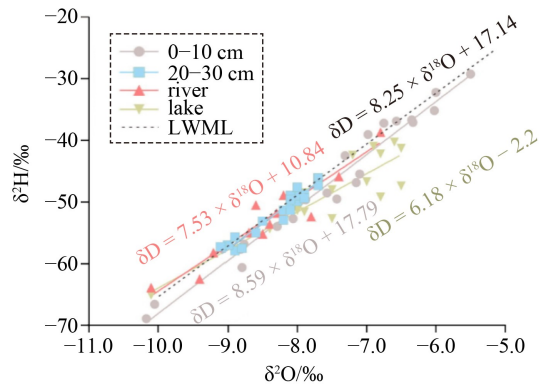


Fig. 5 Plots of $\delta^2\text{H}$ versus $\delta^{18}\text{O}$ in diverse water pools.

Dajiuhu peatland, most rainfall in a single year (around 80%) occurs during the rainy season (April to October). The mean $\delta^2\text{H}_p$ in this period was -65‰ in Dajiuhu (Pu, 2018), which is close to the $\delta^2\text{H}_{pw}$ beneath 50 cm. This indicates that the $\delta^2\text{H}_{pw}$ at deeper depths (50–60, 80–90, 100–110, 120–130, 150–160 cm) is mainly affected by the mixing of the rainy season $\delta^2\text{H}_p$. However, the near-constant $\delta^2\text{H}_{pw}$ at deeper depths over five years suggests that the peat pore water at deeper depths may be affected by multiple years instead of one year, which needs to be proved in future research. Therefore, only the characteristics of surface $\delta^2\text{H}_{pw}$ are discussed in the following part due to the limited variations of the $\delta^2\text{H}_{pw}$ in other peat depths.

The $\delta^2\text{H}_{0-10\text{ cm}}$ among the different monitoring sites in the Dajiuhu peatland showed only minimal deviation, with the variance staying below 12‰ from 2015 to 2019 (Table 2). The close correlations and slight variance

among monitoring sites suggest similar controlling factors. A relatively small variance was also observed in the surface soil $\delta^2\text{H}_{sw}$ in forest, karst hillslope and agricultural fields (Goldsmith et al., 2019; Liu et al., 2022c; Xu et al., 2022). However, the mean $\delta^2\text{H}_{0-10\text{ cm}}$ (ranging from -12‰ to -32‰ , with an average value of -19‰) in the Dajiuhu peatland is smaller than that in other locations, likely due to the similar microtopography and high moisture content. Liu et al. (2022c) observed that the ranges of surface $\delta^2\text{H}_{sw}$ in dry seasons were larger than that in wet seasons. In contrast, the ranges of $\delta^2\text{H}_{0-10\text{ cm}}$ in the Dajiuhu peatland do not show similar seasonal variations and large ranges may occur in both wet seasons and dry seasons (Fig. 3, Table 2), likely due to the high water table in peatlands.

4.2 Controls on seasonal variations of $\delta^2\text{H}_{pw}$

Precipitation is typically the main source of peat pore water. In Dajiuhu, the seasonal variations of $\delta^2\text{H}_{0-10\text{ cm}}$ are reflective of the fluctuations in precipitation, with higher values in the spring (April, May) and lower values in the summer (June, July) (Fig. 6). This decrease is linked to the summer monsoon bringing in moisture with depleted deuterium from the tropical Indian Ocean and the western Pacific Ocean to central China (Tan, 2014). Autumn precipitation also contributes a moderate amount of rain to the area (Ding and Wang, 2008), resulting in relatively lower $\delta^2\text{H}_p$ and $\delta^2\text{H}_{0-10\text{ cm}}$.

The influence of precipitation on $\delta^2\text{H}_{0-10\text{ cm}}$ is not immediate. A previous study found a time lag of 1–3 months between $\delta^2\text{H}_{sw}$ in shallow soil (0–60 cm) and $\delta^2\text{H}_p$ in Changsha (Dai et al., 2020). In the Dajiuhu peatland, it is assumed that $\delta^2\text{H}_{0-10\text{ cm}}$ lags $\delta^2\text{H}_p$ by approximately one month. This is supported by the fact that $\delta^2\text{H}_{0-10\text{ cm}}$ decreases after early summer (June), which is a month later than the variations of $\delta^2\text{H}_p$. Additionally, $\delta^2\text{H}_{0-10\text{ cm}}$ is strongly correlated with the preceding month's $\delta^2\text{H}_p$ in the nearby area ($\delta^2\text{H}_p$ near the Heshang cave, $r = 0.73$, $p < 0.01$, $n = 15$; $\delta^2\text{H}_p$ near the Furong cave, $r = 0.68$, $p < 0.001$, $n = 23$) as opposed to the parallel-month $\delta^2\text{H}_p$ ($r < 0.29$, $p > 0.05$ for both sites) (Wang et al., 2020; Qiu et al., 2021). Furthermore, the $\text{lc-excess}_{0-10\text{ cm}}$ is significantly correlated with the subtraction of the preceding month's $\delta^2\text{H}_p$ from $\delta^2\text{H}_{0-10\text{ cm}}$ in 2016 ($r = -0.76$, $p < 0.05$, $n = 7$) ($\delta^2\text{H}_p$ collected from Pu (2018)).

Accumulating evidence has shown that $\delta^2\text{H}_p$ in the East Asian summer monsoon influenced areas is likely to be impacted more by regional conditions, such as the convective activities in the moisture source regions, rather than local meteorological conditions (Ruan et al., 2019; Wang et al., 2020). A similar trend may exist for the $\delta^2\text{H}_{0-10\text{ cm}}$ in the Dajiuhu peatland, since correlations between $\delta^2\text{H}_{0-10\text{ cm}}$ and local meteorological conditions (temperature, precipitation and RH) are weak (Fig. 7).

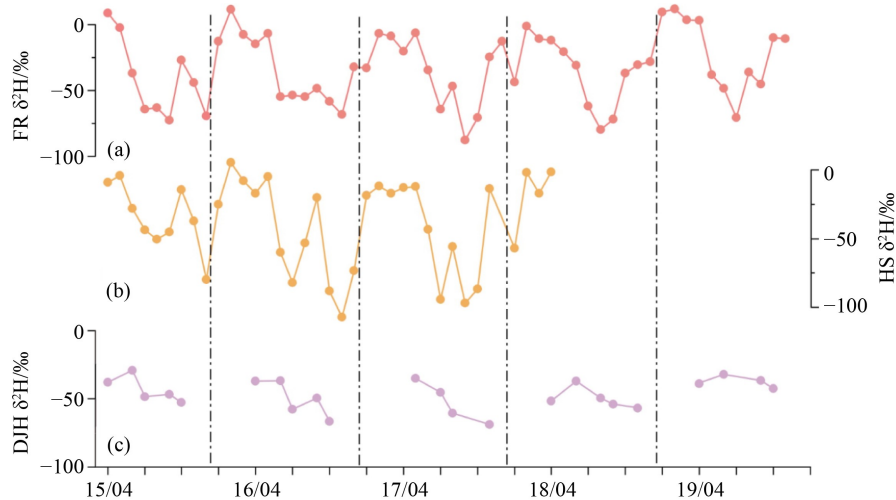


Fig. 6 Variations of $\delta^2\text{H}_p$ in the adjacent areas and $\delta^2\text{H}_{0-10\text{ cm}}$ in the Dajiuhu peatland between 2015 and 2019. (a) monthly $\delta^2\text{H}_p$ near the Furong cave; $\delta^2\text{H}$ is calculated from $\delta^{18}\text{O}$ according to the LWML: $\delta^2\text{H} = 9.07 \times \delta^{18}\text{O} + 21.33$ (Qiu et al., 2021). (b) monthly $\delta^2\text{H}_p$ near the Heshang cave (Wang et al., 2020); $\delta^2\text{H}$ is calculated from $\delta^{18}\text{O}$ according to the LWML: $\delta^2\text{H} = 8.25 \times \delta^{18}\text{O} + 17.14$ (Wang, 2021). (c) Dajiuhu $\delta^2\text{H}_{0-10\text{ cm}}$.

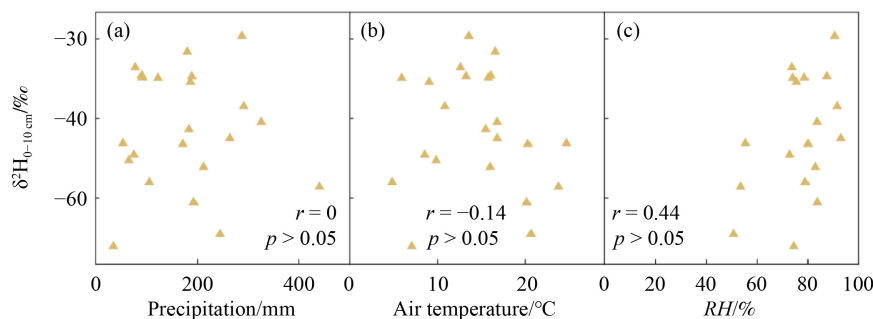


Fig. 7 Correlations between $\delta^2\text{H}_{pw}$ and pre-monthly meteorological data between 2015 and 2019. (a) $\delta^2\text{H}_{0-10\text{ cm}}$ and precipitation. (b) $\delta^2\text{H}_{0-10\text{ cm}}$ and air temperature. (c) $\delta^2\text{H}_{0-10\text{ cm}}$ and the RH.

The temporal variations of $\delta^2\text{H}_{0-10\text{ cm}}$ are largely determined by the isotope composition of precipitation, but the effects of evaporation should not be overlooked. This is evidenced by the reduced values of $\text{lc-excess}_{0-10\text{ cm}}$, which suggests the enrichment of $\delta^2\text{H}_{sw}$ due to evaporation (Sprenger et al., 2016; Liu et al., 2022b; Xu et al., 2022; Liu et al., 2023), from July to September. For example, the high temperature, low precipitation and RH in August and September 2016 caused a severe drought, which is supported by the lowest $\text{lc-excess}_{0-10\text{ cm}}$ during 2016 and a quite positive $\delta^2\text{H}_{0-10\text{ cm}}$ in September 2016. Furthermore, the influence of soil evaporation has been documented in sedimentary $\delta^2\text{H}_{alk}$ (Huang et al., 2018).

The El Niño-Southern Oscillation (ENSO) is believed to be a major factor influencing the yearly variations of $\delta^2\text{H}_{0-10\text{ cm}}$. During El Niño years, the $\delta^2\text{H}_{0-10\text{ cm}}$ tends to be more positive (avg. -43‰ in 2015; -38‰ in 2019) than in other years (avg. -53‰ – -50‰ in 2016, 2017, 2018). Studies have suggested that El Niño activity has an effect on $\delta^2\text{H}_p$ (Sun et al., 2018; Tian et al., 2021). This is because El Niño years tend to have a higher proportion of non-summer monsoon precipitation accounts (around

50% in Jiangxi province), leading to higher $\delta^2\text{H}_p$ (Zhang et al., 2020; Tian et al., 2021). However, the percentage of monsoon precipitation (May to September) in the Dajiuhu peatland remained constant during 2015–2019 (60%–70%). This is likely due to the fact that the Dajiuhu peatland is located near the edge of persistent spring rain areas. Monitoring of $\delta^2\text{H}_p$ near the Heshang cave, which is approximately 100 km from the Dajiuhu peatland, has suggested that the convection and precipitation in moisture source regions can be affected by ENSO (Wang et al., 2020). However, it should be noted that the limited time coverage of this study restricts the ability to compare yearly averaged $\delta^2\text{H}_{0-10\text{ cm}}$ to the ENSO activity on an annual timescale.

4.3 Implications for the application of $\delta^2\text{H}_{alk}$ in peat deposits

Soil water is generally the main water source used by plants for leaf wax synthesis. Thus, the influence of evaporation on $\delta^2\text{H}_{pw}$ may finally be recorded in the $\delta^2\text{H}_{alk}$ (Hou et al., 2008; Yao and Liu, 2014; Herrmann

et al., 2017). The spatial distributions of $\delta^2\text{H}_{\text{pw}}$ in the Dajiuhu peatland suggest that the evaporative enrichment of $\delta^2\text{H}_{\text{pw}}$ is mainly present in the surface peat. However, the effect of soil evaporation on the $\delta^2\text{H}_{\text{alk}}$ of vascular plants is likely to be weak, as their root depths are usually deeper than 10 cm (Huang and Meyers, 2019). Furthermore, the leaf water $\delta^2\text{H}$ of typical vascular plants was found to be close to the $\delta^2\text{H}_{\text{pw}}$ below 50 cm, unaffected by evaporation (Huang and Meyers, 2019). As for *Sphagnum*, another dominant peat-forming plant in Dajiuhu and northern peatlands, although the exact mechanism is still unclear, it appears that soil evaporation does not significantly influence *Sphagnum* $\delta^2\text{H}_{\text{alk}}$.

In the Dajiuhu peatland, the $\delta^2\text{H}_{\text{wax}}$ of peat-forming plants was investigated in two batches of samples, the first collected in September 2016 (Zhao et al., 2018) and the second in August 2017 (Huang and Meyers, 2019). Previous research has indicated that leaf wax synthesis in deciduous trees occurs during the initial period of the growing season (Kahmen et al., 2011; Tipple et al., 2013). This is further evidenced by the fact that, after the initial synthesis, the $\delta^2\text{H}_{\text{wax}}$ remained constant despite any damage to the leaf waxes (Tipple et al., 2013). However, it has been observed that leaf wax can be synthesized throughout the growing season of grasses (Gao et al., 2012), as supported by the grass $\delta^2\text{H}_{\text{wax}}$ data from Dajiuhu (Xue et al., 2022). Thus, it is valid to compare the $\delta^2\text{H}_{\text{wax}}$ with $\delta^2\text{H}_{\text{pw}}$ during the leaf wax synthesis period. The $\delta^2\text{H}_{\text{wax}}$ results of *Euphorbia esula* and *Sanguisorba officinalis* suggest that evapotranspiration has an influence, as the $\delta^2\text{H}_{\text{wax}}$ ($\sim -204\text{‰}$) in 2017 was more negative than in 2016 ($\sim -170\text{‰}$; Zhao et al., 2018; Huang and Meyers, 2019). The differences in $\delta^2\text{H}_{\text{wax}}$ exceeded the differences in $\delta^2\text{H}_{\text{pw}}$ between September 2016 and August 2017 by about 23‰ for $\delta^2\text{H}_{0-10\text{ cm}}$ and 30‰ for $\delta^2\text{H}_{20-30\text{ cm}}$ (Fig. 3). This indicates that the variations in $\delta^2\text{H}_{\text{pw}}$ could not explain the large variations in $\delta^2\text{H}_{\text{wax}}$. One possible reason is the influence of transpiration. The intense drought in September 2016 (Fig. 2) may have caused strong evapotranspiration, leading to the enrichment of leaf water $\delta^2\text{H}$ and more positive $\delta^2\text{H}_{\text{wax}}$. The high water table in the Dajiuhu peatland appears to limit the depth at which the isotope composition of pore water is affected by soil evaporation, and the $\delta^2\text{H}_{\text{alk}}$ of both vascular plants and *Sphagnum* in peatlands may be less affected by soil evaporation. However, long-term drying and severe drought may still affect $\delta^2\text{H}_{\text{alk}}$ through evapotranspiration in peat deposits (Huang et al., 2018; Wang et al., 2022).

The seasonal variation of $\delta^2\text{H}_{0-10\text{ cm}}$ in Dajiuhu reflected the seasonal variation of $\delta^2\text{H}_{\text{p}}$, though this characteristic was weakened with increasing depth due to the mixing of precipitation from the rainy season. $\delta^2\text{H}_{\text{pw}}$ may capture $\delta^2\text{H}_{\text{p}}$ changes over a period of months or even years (Dai et al., 2022). Similarly, $\delta^2\text{H}_{\text{alk}}$ can record changes over longer timescales when water is taken from

deep peat. Nevertheless, this does not impede the interpretation of sedimentary $\delta^2\text{H}_{\text{alk}}$ in peat deposits, since the temporal resolution is usually decades or even centuries for most studies.

5 Conclusions

To explore the spatiotemporal variations of $\delta^2\text{H}_{\text{pw}}$ and the possible controlling factors, peat pore water samples were collected from the Dajiuhu peatland from 2015 to 2019. The main findings are as follows.

1) The amplitude and values of $\delta^2\text{H}_{\text{pw}}$ decrease significantly from -47‰ to -56‰ with increasing depth, and remain relatively constant in the deeper layers with a variance ranging from 11‰ to 2‰. This depth pattern is likely due to the effect of evaporation in the upper layers (0–10, 20–30 cm) and the mixing signal of multiple precipitation events in deeper depths (> 50 cm), which is further highlighted by the deviation between $\delta^2\text{H}_{0-10\text{ cm}}$ and the LMWL in the dual-isotope plot.

2) Precipitation isotope composition is the primary factor influencing the temporal variations of $\delta^2\text{H}_{0-10\text{ cm}}$. The seasonal variations of $\delta^2\text{H}_{0-10\text{ cm}}$ are in agreement with the $\delta^2\text{H}_{\text{p}}$ in the adjacent areas, as evidenced by a strong correlation (1-month preceding $\delta^2\text{H}_{\text{p}}$ near the Heshang cave, $r = 0.73$, $p < 0.01$, $n = 15$; 1-month preceding $\delta^2\text{H}_{\text{p}}$ near the Furong cave, $r = 0.68$, $p < 0.001$, $n = 23$).

3) The $\delta^2\text{H}_{0-10\text{ cm}}$ was relatively high (averaging -43‰ in 2015 and -38‰ in 2019) during El Niño years, indicating that the interannual variations of $\delta^2\text{H}_{0-10\text{ cm}}$ may be associated with ENSO activities; however, a more extended time series is necessary to verify this possibility.

Leaf wax $\delta^2\text{H}$ primarily reflects regional precipitation isotope signals, along with the impact of soil evaporation in the Dajiuhu peatland. Therefore, it can be used to monitor hydroclimate changes in subtropical climates, as evidenced by the large positive excursions of leaf wax $\delta^2\text{H}$ during the dry period in the mid-Holocene in central China (Huang et al., 2018) and the mid-to-late Holocene transition on the south-east coast of China (Wang et al., 2022).

Data availability statement Further inquiries can be directed to the corresponding author.

Author contributions XH designed the study. YW and XH collected samples, performed analyses, and analyzed the data, and wrote the manuscript.

Acknowledgments We thank Zhiqi Zhang, Dr. Jiantao Xue, Bingyan Zhao, Dr. Yiming Zhang, Chaoyang Yan, Xiaofang Yu, Ruicheng Wang, Guang Yang and Xin Yang for their help in the fieldwork. Dr. Xiuli Li and Yingzhao Wang are thanked for their helps in the water isotope analysis. We thanked the anonymous reviewers for their comments to improve the quality of this manuscript. This work was supported by the National Natural Science Foundation of China (Grant No. U20A2094).

References

- Allen S, Brooks J, Keim R, Bond B, McDonnell J (2014). The role of pre-event canopy storage in throughfall and stemflow by using isotopic tracers. *Ecohydrology*, 7(2): 858–868
- Dai J, Zhang X, Luo Z, Wang R, Liu Z, He X, Rao Z, Guan H (2020). Variation of the stable isotopes of water in the soil-plant-atmosphere continuum of a *Cinnamomum camphora* woodland in the East Asian monsoon region. *J Hydrol (Amst)*, 589: 125199
- Dai J, Zhang X, Wang L, Luo Z, Wang R, Liu Z, He X, Rao Z, Guan H (2022). Seasonal isotopic cycles used to identify transit times and the young water fraction within the critical zone in a subtropical catchment in China. *J Hydrol (Amst)*, 612: 128138
- Dawson T (1993). Hydraulic lift and water use by plants: implications for water balance, performance and plant-plant interactions. *Oecologia*, 95(4): 565–574
- Ding Y, Wang Z (2008). A study of rainy seasons in China. *Meteorol Atmos Phys*, 100(1–4): 121–138
- Feakins S, Sessions A (2010). Controls on the D/H ratios of plant leaf waxes in an arid ecosystem. *Geochim Cosmochim Acta*, 74(7): 2128–2141
- Gao L, Burnier A, Huang Y (2012). Quantifying instantaneous regeneration rates of plant leaf waxes using stable hydrogen isotope labeling. *Rapid Commun Mass Spectrom*, 26(2): 115–122
- Gibson J, Birks S, Edwards T (2008). Global prediction of δ_A and $\delta^2\text{H}$ - $\delta^{18}\text{O}$ evaporation slopes for lakes and soil water accounting for seasonality. *Global Biogeochem Cycles*, 22(2): GB2031
- Goldsmith G, Allen S, Braun S, Engbersen N, González - Quijano C, Kirchner J, Siegwolf R (2019). Spatial variation in throughfall, soil, and plant water isotopes in a temperate forest. *Ecohydrology*, 12(2): e2059
- Herrmann N, Boom A, Carr A, Chase B, West A, Zabel M, Schefuß E (2017). Hydrogen isotope fractionation of leaf wax *n*-alkanes in southern African soils. *Org Geochem*, 109: 1–13
- Hou J, D'Andrea W, Huang Y (2008). Can sedimentary leaf waxes record D/H ratios of continental precipitation? Field, model, and experimental assessments. *Geochim Cosmochim Acta*, 72(14): 3503–3517
- Huang X, Meyers P A (2019). Assessing paleohydrologic controls on the hydrogen isotope compositions of leaf wax *n*-alkanes in Chinese peat deposits. *Palaeogeogr Palaeoclimatol Palaeoecol*, 516: 354–363
- Huang X, Pancost R D, Xue J, Gu Y, Evershed R P, Xie S (2018). Response of carbon cycle to drier conditions in the mid-Holocene in central China. *Nat Commun*, 9(1): 1369
- Huang X, Zhang H, Griffiths M L, Zhao B, Pausata F S R, Tabor C, Shu J, Xie S (2023). Holocene forcing of East Asian hydroclimate recorded in a subtropical peatland from southeastern China. *Clim Dyn*, 60(3–4): 981–993
- Huang X, Zhang Z, Wang H, Chen X, Zhu Z, Gu Y, Qin Y, Liu J, Wang Y (2017). Overview on critical zone observatory at Dajiuhu Peatland, Shennongjia. *Earth Sci (Paris)*, 42: 1026–1038 (in Chinese)
- Jung Y, Shin W, Seo K, Koh D, Ko K, Lee K (2022). Spatial distributions of oxygen and hydrogen isotopes in multi-level groundwater across South Korea: a case study of mountainous regions. *Sci Total Environ*, 812: 151428
- Kahmen A, Dawson T, Vieth A, Sachse D (2011). Leaf wax *n*-alkane δD values are determined early in the ontogeny of *Populus trichocarpa* leaves when grown under controlled environmental conditions: early determination of leaf wax *n*-alkane δD values. *Plant Cell Environ*, 34(10): 1639–1651
- Kahmen A, Hoffmann B, Schefuß E, Arndt S, Cernusak L, West J, Sachse D (2013). Leaf water deuterium enrichment shapes leaf wax *n*-alkane δD values of angiosperm plants II: observational evidence and global implications. *Geochim Cosmochim Acta*, 111: 50–63
- Landwehr J, Coplen T (2006). Line-conditioned excess: a new method for characterizing stable hydrogen and oxygen isotope ratios in hydrologic systems. In: *International Conference on Isotopes in Environmental Studies*. Vienna: IAEA, 132–135
- Liu H, Liu W (2019). Hydrogen isotope fractionation variations of *n*-alkanes and fatty acids in algae and submerged plants from Tibetan Plateau lakes: implications for palaeoclimatic reconstruction. *Sci Total Environ*, 695: 133925
- Liu J, An Z (2018). A hierarchical framework for disentangling different controls on leaf wax δD -alkane values in terrestrial higher plants. *Quat Sci Rev*, 201: 409–417
- Liu J, An Z (2019). Variations in hydrogen isotopic fractionation in higher plants and sediments across different latitudes: implications for paleohydrological reconstruction. *Sci Total Environ*, 650: 470–478
- Liu J, Jiang C, Guo L, Hu J (2022b). Ecohydrological separation in a pair catchments covered with natural grassland and planted forestland on the Chinese Loess Plateau: evidence from a one-year stable isotope observation. *Hydrol Processes*, 36(12): e14778
- Liu J, Jiang C, Wu H, Guo L, Zhang H, Zhao Y (2023). Controls on leaf water hydrogen and oxygen isotopes: a local investigation across seasons and altitude. *Hydrol Earth Syst Sci*, 27(2): 599–612
- Liu J, Zhao J, He D, Huang X, Jiang C, Yan H, Lin G, An Z (2022a). Effects of plant types on terrestrial leaf wax long-chain *n*-alkane biomarkers: implications and paleoapplications. *Earth Sci Rev*, 235: 104248
- Liu Q, Wang T, Liu C, Mikouendanandi E, Chen X, Peng T, Zhang L (2022c). Characterizing the spatiotemporal dynamics of shallow soil water stable isotopic compositions on a karst hillslope in southwestern China. *J Hydrol (Amst)*, 610: 127964
- Liu W, Huang Y (2005). Compound specific D/H ratios and molecular distributions of higher plant leaf waxes as novel paleoenvironmental indicators in the Chinese Loess Plateau. *Org Geochem*, 36(6): 851–860
- Liu W, Yang H (2008). Multiple controls for the variability of hydrogen isotopic compositions in higher plant *n*-alkanes from modern ecosystems. *Glob Change Biol*, 14(9): 2166–2177
- McFarlin J, Axford Y, Masterson A, Osburn M (2019). Calibration of modern sedimentary $\delta^2\text{H}$ plant wax-water relationships in Greenland lakes. *Quat Sci Rev*, 225: 105978
- Pu H (2018). Study on the Characteristics of Hydrogen and Oxygen Stable Isotopes in Precipitation of Dajiuhu in Shennongjia and Its Moisture Sources. Dissertation for Master's Degree. Nanjing: Nanjing Normal University (in Chinese)

- Pu H, Song W, Wu J (2020). Using soil water stable isotopes to investigate soil water movement in a water conservation forest in Hani Terrace. *Water*, 12(12): 3520
- Qiu H, Li T, Chen C, Huang R, Wang T, Wu Y, Xiao S, Xu Y, Huang Y, Zhang J, Yang Y, Li J (2021). Significance of active speleothem $\delta^{18}\text{O}$ at annual-decadal timescale—a case study from monitoring in Furong Cave. *Appl Geochem*, 126: 104873
- R Core Team (2022). R: A language and environment for statistical computing. R Foundation for Statistical Computing, Vienna, Austria
- Rao Z, Li Y, Zhang J, Jia G, Chen F (2016). Investigating the long-term palaeoclimatic controls on the δD and $\delta^{18}\text{O}$ of precipitation during the Holocene in the Indian and East Asian monsoonal regions. *Earth Sci Rev*, 159: 292–305
- Ruan J, Zhang H, Cai Z, Yang X, Yin J (2019). Regional controls on daily to interannual variations of precipitation isotope ratios in Southeast China: implications for paleomonsoon reconstruction. *Earth Planet Sci Lett*, 527: 115794
- Sachse D, Billault I, Bowen G, Chikaraishi Y, Dawson T, Feakins S, Freeman K, Magill C, McInerney F, van der Meer M, Polissar P, Robins R, Sachs J, Schmidt H L, Sessions A, White J, West J, Kahmen A (2012). Molecular paleohydrology: interpreting the hydrogen-isotopic composition of lipid biomarkers from photosynthesizing organisms. *Annu Rev Earth Planet Sci*, 40(1): 221–249
- Seki O, Meyers P A, Yamamoto S, Kawamura K, Nakatsuka T, Zhou W, Zheng Y (2011). Plant-wax hydrogen isotopic evidence for postglacial variations in delivery of precipitation in the monsoon domain of China. *Geology*, 39(9): 875–878
- Sprenger M, Leister H, Gimbel K, Weiler M (2016). Illuminating hydrological processes at the soil-vegetation-atmosphere interface with water stable isotopes. *Rev Geophys*, 54(3): 674–704
- Sun Z, Yang Y, Zhao J, Tian N, Feng X (2018). Potential ENSO effects on the oxygen isotope composition of modern speleothems: observations from Jiguan Cave, central China. *J Hydrol (Amst)*, 566: 164–174
- Tan M (2014). Circulation effect: response of precipitation $\delta^{18}\text{O}$ to the ENSO cycle in monsoon regions of China. *Clim Dyn*, 42(3–4): 1067–1077
- Tian Y, Zhang H, Zhang R, Zhang F, Liang Z, Cai Y, Cheng H (2021). Seasonal and inter-annual variations of stable isotopic characteristics of rainfall and cave water in Shennong Cave, southeast China, and its paleoclimatic implication. *Front Earth Sci (Lausanne)*, 9: 794762
- Tipple B, Berke M, Doman C, Khachatryan S, Ehleringer J R (2013). Leaf-wax *n*-alkanes record the plant–water environment at leaf flush. *Proc Natl Acad Sci USA*, 110(7): 2659–2664
- Wang X, Huang X, Zhao H, Sachse D (2022). Abrupt drying on the southeast coast of China during the mid- to late-Holocene transition. *Geophys Res Lett*, 49: e2022GL100257
- Wang Y (2021). Temporal and Spatial Evolution of Precipitation Stable Isotopes in Western Hubei: Implications for Palaeoclimate and Paleoaltimetry Reconstruction. Dissertation for Doctoral Degree. Wuhan: China University of Geosciences (in Chinese)
- Wang Y, Hu C, Ruan J, Johnson K R (2020). East Asian precipitation $\delta^{18}\text{O}$ relationship with various monsoon indices. *J Geophys Res Atmos*, 125(13): e2019JD032282
- Wang Z, Liu W, Wang H, Cao Y, Hu J, Dong J, Lu H, Wang H, Xing M, Liu H (2021). New chronology of the Chinese loess-paleosol sequence by leaf wax δD records during the past 800 k. y. *Geology*, 49(7): 847–850
- Wei T, Simko V (2021). R package ‘corrplot’: visualization of a correlation matrix (Version 0.92)
- Xie S, Nott C J, Avsejs L A, Volders F, Maddy D, Chambers F M, Gledhill A, Carter J F, Evershed R P (2000). Palaeoclimate records in compound-specific δD values of a lipid biomarker in ombrotrophic peat. *Org Geochem*, 31(10): 1053–1057
- Xu M, Liu Q, Wu D, Wang T, Espoire M, Chai Q (2022). Characterization of spatiotemporal patterns of soil water stable isotopes at an agricultural field. *Sci Total Environ*, 828: 154538
- Xue J, Zhang X, Li J, Zhang Z, Yao H (2022). Seasonal variations of leaf wax *n*-alkane distributions and $\delta^2\text{H}$ values in peat-forming vascular plants from the Dajiuhe peatland, central China. *Front Earth Sci*, 16(3): 774–785
- Yang G, Zhang Y, Huang X (2024). Fluctuations of water table level in a subtropical peatland, central China. *J Earth Sci*
- Yang Y, Zhang Y, Zhang H, Huang X (2023). Quantitative reconstruction of the relative humidity by a coupled $\delta^{18}\text{O}$ - $\delta^2\text{H}$ approach during the Younger Dryas in central China. *Quat Sci Rev*, 299: 107879
- Yao Y, Liu W (2014). Hydrogen isotopic composition of plant leaf wax in response to soil moisture in an arid ecosystem of the northeast Qinghai-Tibetan Plateau, China. *J Arid Land*, 6(5): 592–600
- Zhang H, Cheng H, Cai Y, Spötl C, Sinha A, Kathayat G, Li H (2020). Effect of precipitation seasonality on annual oxygen isotopic composition in the area of spring persistent rain in southeastern China and its paleoclimatic implication. *Clim Past*, 16(1): 211–225
- Zhang Y, Huang X, Zhang Z, Blewett J, and Naafs B D A (2022). Spatiotemporal dynamics of dissolved organic carbon in a subtropical wetland and their implications for methane emissions. *Geoderma*, 419: 115876
- Zhao B, Hu J, Shu J, Huang X (2022). Early onset of summer monsoon during the Mystery Interval (17.5–14.5 ka BP) in the East Asian Summer Monsoon area: evidence from leaf alkane $\delta^2\text{H}$. *Quat Sci Rev*, 294: 107757
- Zhao B, Zhang Y, Huang X, Qiu R, Zhang Z, Meyers P A (2018). Comparison of *n*-alkane molecular, carbon and hydrogen isotope compositions of different types of plants in the Dajiuhe peatland, central China. *Org Geochem*, 124: 1–11
- Zhao C, Rohling E J, Liu Z Y, Yang X Q, Zhang E, Cheng J, Liu Z H, An Z, Yang X D, Feng X, Sun X, Zhang C, Yan T, Long H, Yan H, Yu Z, Liu W, Yu S Y, Shen J (2021). Possible obliquity-forced warmth in southern Asia during the last glacial stage. *Sci Bull (Beijing)*, 66(11): 1136–1145